International Journal of Refrigeration 154 (2023) 33–42

Contents lists available at ScienceDirect

International Journal of Refrigeration

journal homepage: www.elsevier.com/locate/ijrefrig

Experimental assessment of low temperature phase change materials (PCM) for refrigerating and air conditioning applications

Évaluation expérimentale des matériaux à changement de phase à basse température pour les applications de froid et de conditionnement d'air

Dario Guarda, Giulia Righetti *, Giovanni A. Longo, Claudio Zilio, Simone Mancin

Department of Management and Engineering, University of Padova, Vicenza 36100, Italy

ARTICLE INFO

Keywords:
Low-temperature PCM
Latent thermal energy storages
Paraffin waxes
Melting
Freezing
Corrosion

Mots clés:
Matériaux à changement de phase à basse temperature
Stockage d'énergie thermique latent
Cires de paraffine
Fusion
Congélation
Corrosion

ABSTRACT

Refrigeration, air conditioning and heat pump sector represents between 25 and 30% of the global consumption of electricity and this figure is expected to rapidly grow due to the current trend of electrification. To increase the efficiency of these systems or to maximize the use of renewable energy, latent thermal storage systems are being studied and recommended. However, there is a lack of reliable design rules based on trustable data that could help the thermal experts to design efficient and cost-effective latent thermal energy storage. This paper follows a previous work recently published (Longo et al., 2022) where the thermo-physical and transport properties of a few low temperature PCMs (i.e. 2–9 °C of melting temperature) were measured and discussed. In the present work, the attention is focused on two other fundamental aspects: the PCMs' compatibility with the most common construction materials and their thermal behaviour during the solid/liquid phase change. The collected results will contribute to add currently unavailable data in the literature and to highlight interesting insights on the performance of the selected PCMs.

1. Introduction

In the last few years, the number of publications about Phase Change Materials (PCMs) in the literature is exponentially increasing (Liu et al., 2022). In fact, there is a growing need to efficiently store heat in order to make better use of renewable energy sources, to recover a larger amount of waste heat, and to improve the efficiency of energy systems (Mehling et al., 2022). As compared to current heat storage methods (sensible, thermochemical, and latent) PCMs can provide higher energy density than sensible storages, being easier to be controlled and managed as compared to thermochemical ones.

At the present time, several materials with a wide range of phase change temperatures (i.e., from -20 °C to +500 °C) are available as PCMs (Liu et al., 2022). The ideal PCM should be chemically stable, non-toxic nor explosive, non-corrosive, abundant and cheap. Furthermore, its phase change temperature should be compatible with the operating conditions and the subcooling phenomenon should be negligible. Moreover, its latent heat of fusion and thermal conductivity should be as large as possible while the volume expansion during the melting should be as lower as possible to prevent a potential PCM leakage.

The ideal PCM still does not exist; paraffin waxes are known as one of the best compromises due to good material compatibility, nontoxicity, and relatively high latent heat. Unfortunately, their inherent low thermal conductivity issue is well known, so many enhancement techniques have already been proposed, which are well resumed in the several review papers by (Al-Maghalseh and Mahkamov, 2018; Mahdi et al., 2019; Rehman et al., 2019; Tao and He, 2018).

Currently, many materials having the phase change temperature higher than 20 °C have been considered, and a great number of papers about them have been published. See for instance the reviews by (Al-Maghalseh and Mahkamov, 2018; Kalapala and Devanuri, 2018; Khan et al., 2016; Reddy et al., 2018).

Unfortunately, only little research has been done on PCMs that can

* Corresponding author.
E-mail address: giulia.righetti@unipd.it (G. Righetti).

https://doi.org/10.1016/j.ijrefrig.2023.07.016
Received 3 March 2023; Received in revised form 21 July 2023; Accepted 22 July 2023
Available online 23 July 2023

Nomenclature

Abbreviation

HVAC	heat ventilation and air conditioning
LTES	latent thermal energy storage
PCM	phase change material
PLA	polylactide
PV	photovoltaic
TC	thermocouple
TES	thermal energy storage

Greek symbols

η	efficiency, [-]

Roman symbols

d*t*	temperature difference, [K]
t	temperature, [°C]
T	temperature, [K]

Subscripts

c	condensation
e	evaporation
PC	phase change
PCM	phase change material

be used in low and very-low temperature applications such as heat ventilation and air conditioning (HVAC) systems or applications for the cold chain (Li et al., 2012; Liu et al., 2022; Sarkar et al., 2022; Veerakumar and Sreekumar, 2016). Moreover, a large part of these works deals with frozen products (PCMs at negative temperature) and only a few of them concern the temperature range 2–10 °C, although this temperature range is critical for the cold chain of fresh products and for air conditioning in the residential sector (Calati et al., 2022). Recently, (Longo et al., 2022) measured the thermo-physical and transport properties of 5 PCMs in the temperature range between 2 and 9 °C. In particular, liquid density, heat capacity, dynamic viscosity, and thermal conductivity were presented and discussed.

Among the other few works, almost all deal with PCMs used to store cold energy produced by chillers or cooling systems, often powered by renewable energy sources such as photovoltaic (PV) panels (Dong et al., 2022; Pirdavari and Hossainpour, 2020; Qiao et al., 2019; Rakkappan et al., 2021) or with PCMs directly integrated into the chiller or the refrigerators as proposed by (Maiorino et al., 2019) and other works cited by the (Zhang et al., 2018) review.

1.2. Novelty of this paper

Currently, systematic studies about the main performance characteristics of PCMs with melting temperature in the 2–10 °C range are missing in the open literature. For example, there is a lack of experimental data about the compatibility of these PCMs with the main construction materials. In addition, there are no data comparing the thermal behaviour during charging and discharging of several PCMs in the 2–10 °C range under the same operating conditions. Several research studies have analysed the effects of metal inserts to speed up the phase change process of PCMs, but only few systematic works investigated the effect of different geometries on several PCMs and none of those covered the present materials specifically.

This work analyses the compatibility of seven commercial PCMs in the range 2–9 °C with copper, aluminium, stainless steel, and plastic over a time span of two months. In addition, in this work a systematic experimental campaign was defined and conducted to study in detail the charging and discharging phases of these PCMs inside four 40 × 40 × 60 mm samples. These samples are aluminium boxes having periodical 3D aluminium lattices which were specifically designed to enhance the heat transfer and give interesting insights on the solid/liquid phase change phenomena, which are deeply affected by the thermo-physical and transport properties of the PCM.

The behaviour of the PCMs was compared in terms of total charging/discharging time and temperature field as a function of the lattice geometry and of the bath temperature. This new data add information currently unavailable in the literature and encourage designers to use PCMs in low-temperature applications as well.

2. Material selection

Seven commercial materials with a phase change temperature range from 2 to 9°C were selected. The list of PCMs, the nominal phase change temperature t_{PC}, the PCM type, and the main thermophysical properties are listed in Table 1. Water data are added as a reference. The indicative cost of the PCM is around 10 €/kg, but this could vary depending on the quantity, market and other factors.

The listed thermophysical properties were declared by the manufacturers (Rubitherm and PLUSS Advanced Technologies), but sometimes they slightly differ from those measured experimentally. (Longo et al., 2022) measured a few of those thermophysical and transport properties finding out that sometimes the experimental values are slightly different from the declared ones. In particular, Table 1 also includes the measured liquid thermal conductivity for RT2, RT5, OM5P, OM8, and CR9 to be compared with that declared by the manufacturer. (Longo et al., 2022) also measured the dynamic viscosity of the liquid PCMs above their solidification temperature. The dynamic viscosity is of great importance because it affects the natural motions inside the liquid PCM during the phase change. In fact, a high viscosity inhibits the natural convection and thus it limits the heat transfer during the phase change. Fig. 1 shows the dynamic viscosity of 5 of the seven PCMs estimated using the correlations proposed by Longo et al. (2022).

All the PCMs have a dynamic viscosity greater than that of water and the Crodatherm9.5 presents values which are from 7.4 to 8.3 times higher than water. The OM8 dynamic viscosity is somewhat 3 times higher while those of RT2, RT5, OM5P are 2.2-2.3 times higher.

When compared to water, which is universally recognized for its excellent heat transfer properties and low cost, almost all the PCMs lose attraction. In fact, the ice presents the highest latent heat and thermal conductivity with a great density coupled with the lowest dynamic viscosity, makes it the best PCMs because it exhibits the highest energy density capacity and superior heat transfer capabilities as compared to the selected PMCs. However, the comparison should also include the phase transition temperature because it deeply affects the energy efficiency of the refrigerating or air conditioning equipment that has to be used to produce the cold energy to be stored in the latent thermal energy storage operating with the proposed PCMs.

It is not the scope of this paper to discuss case studies of refrigeration units coupled with latent heat storages. However, it is interesting to take the theoretical example of a Carnot cycle to underline how important it is to select the PCM with the most suitable phase change temperature for each application. It is well known that a Carnot cycle does not take irreversibilities into account and that it is not technically feasible, but it is equally well known that its behaviour reflects that of real cycles and that its efficiency (Eq. (1)), like that of real cycles, increases with the increase in evaporation temperature. Consider the case of a refrigeration unit that has to store cold energy inside a latent storage. Assume (given the ideal case as an example) a Carnot cycle with source at evaporation temperature and sink at condensing temperature. So that, the evaporation temperature of the chiller is equal to the phase change temperature of the PCM (t_{PC}) and keep the evaporator surface area constant. It is possible to select water (t_{PC}=0 °C) or a PCM with t_{PC} = 2 °C. The Carnot efficiency (calculated with the definition in Eq. (1)) increases by 6% (6.83 for the water case versus 7.24 for the 2 °C melting-point PCM). This can lead to substantial primary energy and costs savings, and

Table 1
Main thermophysical properties as declared by the manufacturers. Liquid thermal conductivity measured by Longo et al., (2022) is also reported for comparison purpose.

	H2O/Ice	RT2	savE-OM3	RT4	savE-OM5P	RT5	savE-OM8	CR9
Manufacturer	-	Rubitherm	Pluss	Rubitherm	Pluss	Rubitherm	Pluss	Crodatherm
Type	inorganic	organic, paraffin	organic, fatty acid	organic, paraffin	organic, paraffin	organic, paraffin	organic, fatty acid	organic, vegetable oil
nominal t_{PC} (°C)	0	2	3	4	5	5	8	9
t melting (°C)	0	2	4	4	6	5-6	7	9
t crystallisation (°C)	0	2	3	4	5	5-6	7.8	9
latent heat (kJ/kg)	334	115	229	135	215	230	175	220
density (L) (kg/m^3)	999	770	835	770	763	760	1060	858
density (S) (kg/m^3)	919	880	912	880	727	880	1190	963
specific heat capacity (L) (kJ/kg K)	4.22	2	1.91	2	5.95	2	2.11	2.1
specific heat capacity (S) (kJ/kg K)	2.03	2	1.76	2	3.86	2	1.71	2.2
thermal conductivity (L) (W/m K) (Manufacturer or NIST for water @20 °C)	0.597	0.2	0.146	0.2	0.37	0.2	0.118	0.15
thermal conductivity (L) (W/m K) Longo et al. (2022)@20°C)	0.598	0.169	-	-	0.173	0.163	0.170	0.158
thermal conductivity (S) (W/m K)	2.2	0.2	0.224	0.2	ND	0.2	0.235	0.24

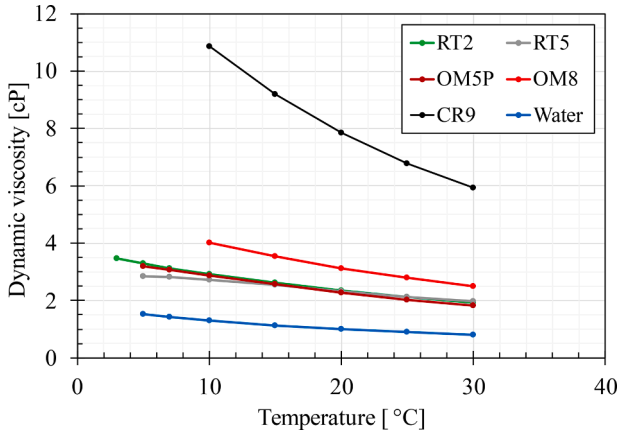

Fig. 1. Estimated dynamic viscosity of 5 different PCM and water as a function of the temperature. Water data from NIST while PCM curves estimated with the model proposed by Longo et al. (2022).

greenhouse gas emissions reduction. This theoretical consideration is useful to highlight the potential of PCM implementation in refrigerating systems.

$$\eta = \frac{T_e}{T_c - T_e} \tag{1}$$

3. Compatibility tests

To design cost-effective, durable, and efficient thermal system, it is of paramount importance to select the most suitable materials in order to avoid any possible incompatibilities that could lead to undesired failures. For this reason, the compatibility of the seven PCMs with aluminium, copper, stainless steel, and a plastic material (polylactide PLA) over a time interval of two months was experimentally studied.

Cylindrical samples having height 50 mm and diameter from 6 to 8 mm were prepared, photographed, and weighed before and after the compatibility test campaign. They were soaked in the PCMs for 2 months and kept in the dark at constant temperature of 25 °C. Table 2 summarizes the weight of the samples before and after the soaking time in the PCM, while Fig. 2 shows a picture of them after the compatibility test. A Mettler Toledo PM6100 scale (± 0.01 g uncertainty) was used to weight the samples.

It can be concluded that the weight remained unchanged except in the case of the PLA sample immersed in OM8 that increased from 2.90 to 4.27 g by absorbing part of the PCM. In addition to this case, the photo shows that copper tends to slightly oxidize when in contact with OM8 and CR9. Thus, OM8 seems to present a noticeable incompatibility with plastics. This means that additional specific compatibility tests are strongly encouraged if OM8 has to work in contact with plastic materials.

4. Experimental set up

Fig. 3 shows the schematic view of the experimental setup. The same volume of each PCM (equal to $6.4 \cdot 10^{-5}$ m^3) was placed inside an aluminium sample having external dimensions 40 × 40 × 60 mm (see Fig. 4 for a drawing of the samples that includes detailed dimensions). An insulated lid was used to prevent any liquid leakage and to limit heat loss to the environment. A few millimetres of air were present between the PCM level and the lid when the PCM was solid, due to the thermal expansion of the material. Two thermostatic baths (Lauda Eco RE620S) fed by a mixture of water and ethylene glycol (70/30% vol.) were used to maintain the selected temperature with a stability of ± 0.02 K.

Table 2
Samples weight expressed in grams before and after the compatibility test.

	PLA		Stainless steel AISI 316L		Al		Cu	
	Before	After	Before	After	Before	After	Before	After
RT2	2.89	2.9	7.78	7.77	10.22	10.22	6.84	6.84
OM3	2.91	2.92	7.65	7.66	10.32	10.31	6.53	6.53
RT4	2.90	2.90	7.73	7.71	10.04	10.04	6.91	6.91
OM5	2.91	2.91	7.81	7.8	10.38	10.37	6.92	6.91
RT5	2.90	2.91	7.80	7.80	10.57	10.57	6.96	6.97
OM8	2.90	4.27	7.46	7.46	10.06	10.05	7.09	7.1
CR9	2.91	2.92	7.95	7.95	9.83	9.82	6.83	6.83

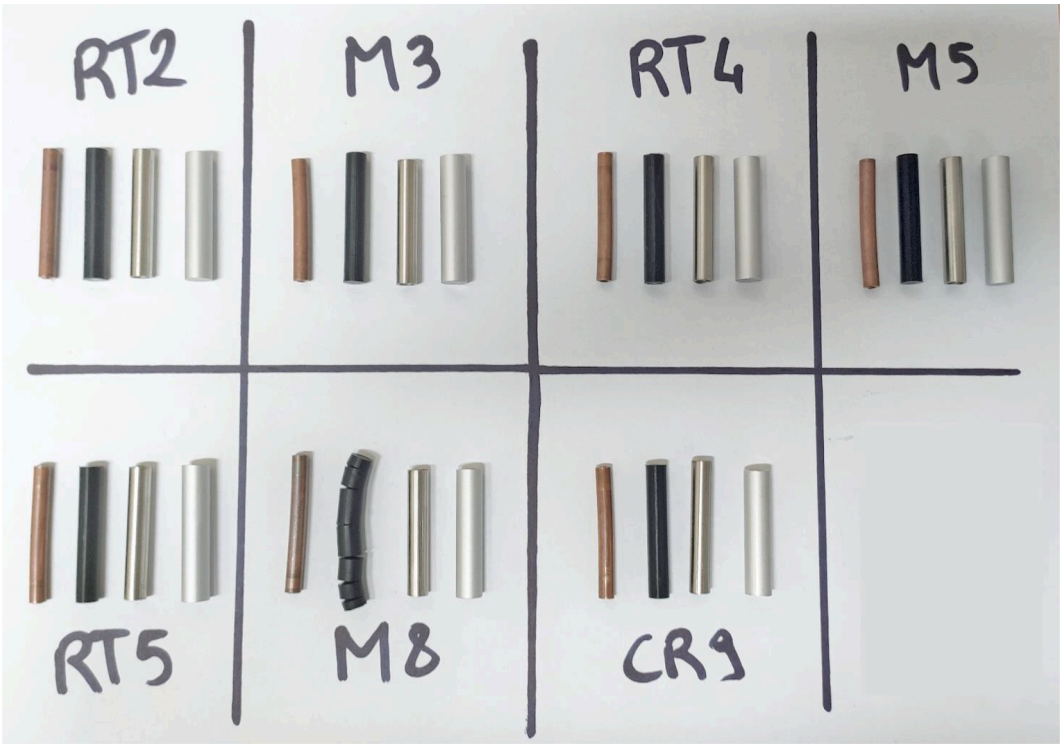

Fig. 2. A picture of the samples after two months of exposure in commercial PCMs.

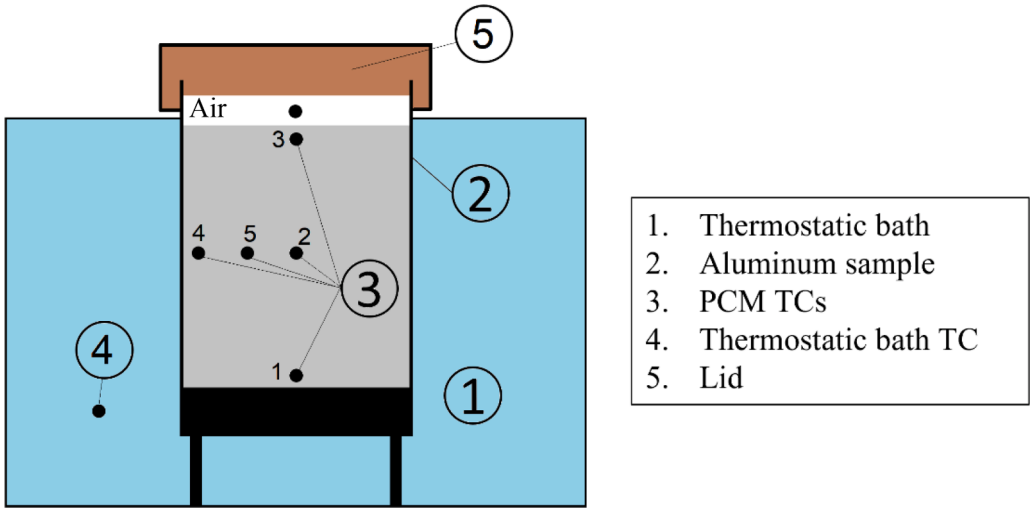

Fig. 3. 2D sketch of the experimental setup.

Four samples were designed and then fabricated via metal additive manufacturing from aluminium alloy AlSi10Mg-0403. Three of them have a 3D periodic lattice structure with a base size of 10, 20 and 40 mm, respectively with a constant porosity (void volume/total sample volume) equal to 0.95, while the fourth is empty. From here on, the samples will be called 10 mm, 20 mm, 40 mm, and reference (the one without lattice structures). These geometries were chosen to increase the average thermal conductivity of the composite system PCM/3D aluminum structure and thus to improve the heat transfer rate. Fig. 4 shows the main dimensions of the four samples. Further details are available in (Righetti et al., 2020a, 2020b).

The PCM temperature distribution was measured by means of 5 T-type thermocouples (uncertainty ±0.1 K, k=2). A sixth T-type thermocouple (named as "air") was placed in the cavity between the lid and the PCM and another was immersed in the thermostatic bath water. Fig. 3 also shows the location of the thermocouples.

Experimental heat transfer tests were conducted on seven commercial PCMs during the charging and discharging phases. The charging phase involved the solidification of the PCM, resulting in cold energy storage, by immersing the sample containing PCM at room temperature in a thermostatic bath set 3, 6, or 9 K colder than t_{PC}. This phase begins when the thermocouples inserted in the PCM are lower than (t_{PC}+8 K) and ends when they are 2 K lower than t_{PC}. The discharging phase is the opposite: it begins when the sample is immersed in a thermostatic bath 3, 6 or 9 K warmer than t_{PC} and ends when the same thermocouples are 2 K warmer than t_{PC} and ends when they are 8 K higher than t_{PC}.

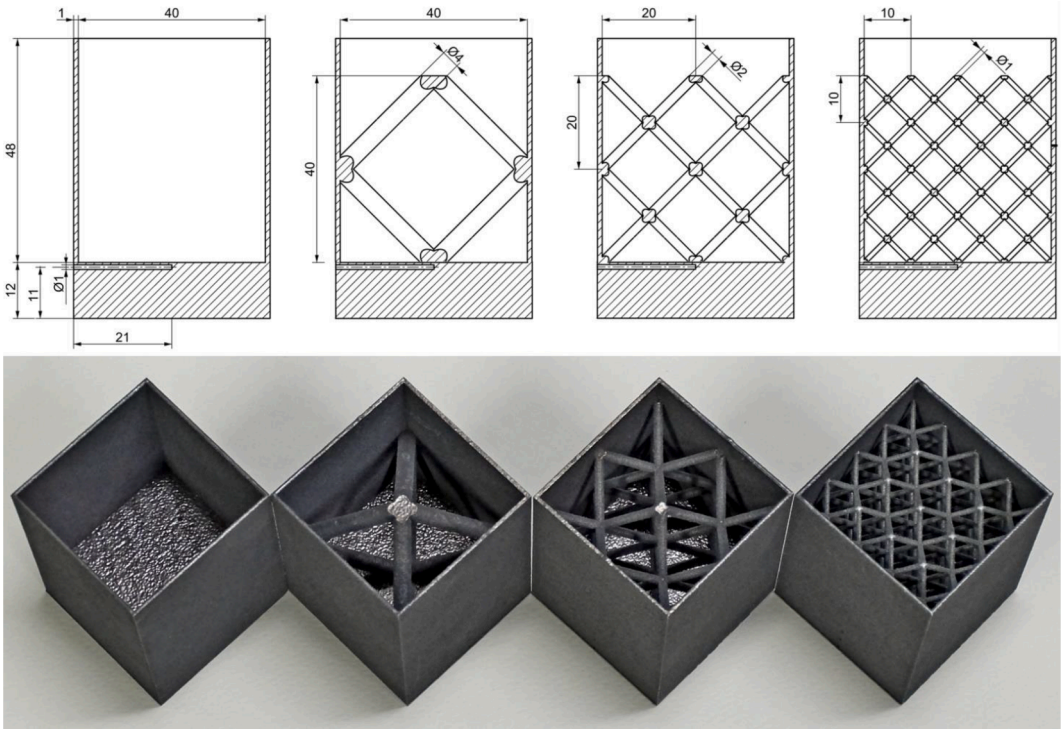

Fig. 4. A scheme of the four samples (top) and a picture of them (bottom).

4. Experimental results

Several new experimental tests were run to investigate the temperature field and the duration of the charging and discharging phases of seven commercial PCMs under different working conditions in four samples. Also water was taken into consideration, as a reference PCM with a nominal phase change temperature of 0 °C.

Before starting the discussion about the phase change processes, it is important to highlight that in the case of low temperature PCMs, differently from what it usually happens with the high temperature ones, the charging phase is the solidification, while the discharging phase is the melting. This is because, the solidification process is related to the cold energy storage while the melting to the cold energy release since the heat transfer fluid is cooled down by transferring heat to the PCM, which melts.

First of all, Tables 3, 4, and 5 resume the total length (in minutes) of all the tested conditions when the temperature difference between t_{PC} and thermostatic bath temperature (dt) is 9, 6, and 3 K, respectively. The densities of the PCMs are different, thus the samples were filled with different amounts of material. For this reason, a direct comparison between the PCMs cannot be conducted because the energy capacity is different. Nonetheless, the behaviour in term of cycles for each material can be compared to highlight the effects of the different thermophysical properties and of the 3D structure.

The first value is the charging time (i.e. solidification), while the second one is the discharging one (i.e. melting), both expressed in minutes.

The data reported in the tables must be analysed in the light of the thermophysical properties reported in Table 1 and Fig. 1. Considering the reference sample, it clearly appears the strong effect of the thermal conductivity in absence of any enhanced surface. In fact, the thermal conductivity of the common PCMs does not vary between liquid and solid, differently, water solid thermal conductivity is around 3.7 times greater than that of the liquid. This translates in the results reported in the first row of Table 3 for the reference empty sample; the water (i.e. ice) is the only PCM for which the charging time, 34', (i.e. solidification)

Table 4
Charging (i.e. solidification) and discharging (i.e. melting) times in minutes of all the tests when dt is 6 K.

dt 6 K	OM5	RT5	OM8	CR9
Reference	131/97	126/106	-	-
40 mm	70/63	71/65	-	-
20 mm	27/40	25/37	-	-
10 mm	18/22	17/23	17/27	21/24

Table 5
Charging (i.e. solidification) and discharging (i.e. melting) times in minutes of all the tests when dt is 3 K.

dt 3 K	RT2	OM3	RT4	OM5	RT5	OM8
Reference	-	-	-	238/288	256/293	-
40 mm	-	-	-	181/153	204/131	-
20 mm	-	-	-	96/96	136/95	-
10 mm	57/30	96/61	42/26	41/39	46/48	38/33

Table 3
Charging (i.e. solidification) and discharging (i.e. melting) times in minutes of all the tests when dt is 9 K.

dt 9 K	H2O	RT2	OM3	RT4	OM5	RT5	OM8	CR9
Reference	34/92	150/51	124/73	117/50	86/62	93/63	101/66	147/68
40 mm	22/67	65/31	76/38	56/31	52/42	51/43	56/32	78/40
20 mm	17/37	18/21	28/26	17/20	14/25	18/25	22/22	33/21
10 mm	13/34	13/10	15/18	10/12	13/14	13/15	15/17	15/15

is remarkably faster (i.e. around 3 times) than discharging (i.e. melting), 92', All the other PCMs present the opposite behaviour with the solidification from 1.3 to 3 times slower than the melting phase. These results can be explained considering that in the case of water/ice, given the high solid thermal conductivity, the conduction is the dominant heat transfer mechanism in both charging and discharging phases. Differently, in the case of the other organic PCMs, as expected, the charging phase was dominated by the solid conduction that is hindered by the low thermal conductivity while the discharging phase is speeded up by the natural convection, which in this case is noticeable. It is worth to point out that the described results were collected at constant operating water bath to PCM temperature difference of 9 K. This means that the driving force of the heat transfer was the same for all the PCMs.

Table 3 also reports the effects of the 3D metal lattice on the heat transfer performance of the PCMs; starting from water, the enhancement increases as the pore size decreases from 10 to 40 mm but the ratio between the charging and discharging phase remains almost constant, meaning that the phase change mechanisms do not vary. The analysis of the results collected for the other 7 PCMs reveals a completely different behaviour; there is a clear enhancement even in the case of 40 mm size 3D lattice, which boosted both the charging and discharging phases with a slightly more improvement of the solidification process where the presence of the thick aluminium fibres improved the conduction through the PCM but the ratio between the two phases (charging over discharging) decreased around 30% being within 1.2 and 2.

When the size of the pore decreased to 20 mm, for RT2, RT4, OM5, and RT5 the charging phase became even faster than the discharging meaning that the enhanced surface was able to counterbalance the low thermal conductivity being even more effective than the natural convection, which is partially suppressed by the 3D structure. This is also confirmed from the analysis of the data for 10 mm sample: the charging phase is faster than the discharging for almost all the PCMs. The CR9 presents a qualitative similar behaviour but quantitatively different. In fact, this bio-based PCM presents the highest dynamic viscosity and, the natural convection is therefore limited even in the empty sample. Hence, the charging phase remains longer than the discharging phase up to a pore size of 10 mm, for which the two phases took the same time. This can be explained considering that the 3D structure enhances both the solidification and melting phases but being so viscous, the CR9 does not experience a great limitation during the melting phase.

When decreasing water bath to PCM temperature difference to 6 K and then to 3 K, the phase change processes are longer because the heat transfer is generally limited. At 6 K, the ratio between the charging and discharging time presents the same behaviour shown at 9 K with values within 1.35 and 0.7. The 10 mm remains the 3D structure which exhibited the best performance in both charging and discharging phases, showing the fastest processes. At 3 K, the phase change processes became even longer; only the 10 mm sample kept the phase change times below 1 h and there were not any noticeable difference between the charging and discharging times.

In general, in 37% of cases, the difference between charging and discharging time is less than 20%. Moreover, considering the 10 mm sample, the discharging time is often longer than the charging time (11 times out of 18). On the other hand, in the reference sample, the discharging time is shorter than the charging time: 9 times out of 12. Therefore, it can be concluded that the presence of the structure speeds up the charging process more than the discharging one. In fact, on average, the charging time is reduced by about 8 times when comparing the 10 mm sample and the reference one, while the discharging time is reduced only by somewhat 4 times.

Therefore, it is likely that under the same operating conditions, the effect of metal structures is stronger when there is a layer of solid material around the walls, which reduces convective effects. In the next paragraphs, material, working conditions, and sample effects will be analysed separately. All the following diagrams report the temperature difference between the average temperature of the PCM, t_{PCM} (average of the 5 thermocouples named from t1 to t5) and t_{PC} as a function of the time.

As already discussed, the reference sample (the one without metallic lattice structures) takes significantly longer melting and solidification times than the others. It takes up to from 2.6 to 11.7 times longer than the 10 mm sample. On the other hand, when comparing different structures, the 10 mm reduces the charging time by about 4.3 times compared to the 40 mm and by about 1.7 times when compared to the 20 mm.

However, not all materials present the same effects in charging time as a function of the 3D periodic structure. At the same dt (equal to 9 K), the PCM that is most sensitive to lattice geometry variation is RT4, which reduces the time by 5.6 times when the 10 mm is used instead of the 40 mm. While CR9 is the most sensitive when 10 mm is used instead of 20 mm, with a time reduction of 2.2 times. In contrast, the least sensitive material to the lattice geometry is water, which reduces the charging time only by 1.7 times passing from 40 to 10 mm and by 1.3 times passing from 20 to 10 mm.

For all materials, the duration of the discharging phase (melting) is less sensitive to the geometry used. On average, the 10 mm reduces the discharging time by about 3.1 times compared to the 40 mm and by about 1.1 times when the 10 mm is compared to the 20 mm. In this case, RT2 is the material that reduces the time the most: 3.1 times in going from 40 to 10 mm and 2.1 times in going from 20 to 10 mm. Once more, water is the substance that shortens the discharge time the least: 2 and 1.1 times in going from 40 to 10 mm and from 20 to 10 mm, respectively.

To run a more detailed analysis, it was chosen to contrast RT4, one of the most sensible materials to the lattice geometry variation, with water, the least sensible one. Water, compared to RT4, has a significantly higher thermal conductivity, so the effects of the 3D structure can be reduced.

Fig. 5 presents the histograms of the time expressed in minutes required by water and RT4 to complete the charging (Fig. 5a) and discharging (Fig. 5b) phases when a dt 9 K is applied.

4.1. *Effect of the material*

The material plays a key role in the charging/discharging time and temperature distribution. Fig. 6a compares the average temperature difference (t_{PCM} - t_{PC}) profiles during charging process of the 7 materials (plus water) in the 20 mm sample when the temperature difference between bath and t_{PC} was kept equal to 9K. Fig. 6b reports the discharging phase.

The higher latent heat materials (water, RT5, OM3, listed in descending order) are expected to take longer phase change times under the same operating conditions. Instead, the tests showed that CR9 is the material with the longest charging time (i.e. 33 min). It is followed by OM3 with 28 min and OM8 with 22. So, it is evident that also other thermophysical properties matter, such as thermal conductivity. For example, water, which has the highest latent heat, due to a thermal conductivity of the solid almost an order of magnitude higher than the other materials takes only 17 min to solidify. Moreover, the 3D structure mitigates the common subcooling effect of the water, which, in this tests, did not show any subcooling at the onset of the solidification.

Considering the three materials produced by Rubitherm (RT2, RT4, and RT5), they are all paraffin waxes and have similar thermophysical properties (see Table 1). Only the latent heat (in addition to t_{PC}) varies: 230 kJ/kg RT5, 135 kJ/kg RT4 and 115 kJ/kg RT2. Despite the different latent heat, charging time is very similar, differing by only 1 min between the three PCMs. In contrast, the temperature trend inside the sample is different during the charging phase. When RT5 is used, a temperature plateau during the phase change is clearly shown, whereas when RT2 and RT4 are used, the average temperature continues to decrease. This might be due to the fact that the latent heat of the RT5 is almost 2 times higher than those of RT2 and RT4.

During the discharging phase, RT2 and RT4 showed similar

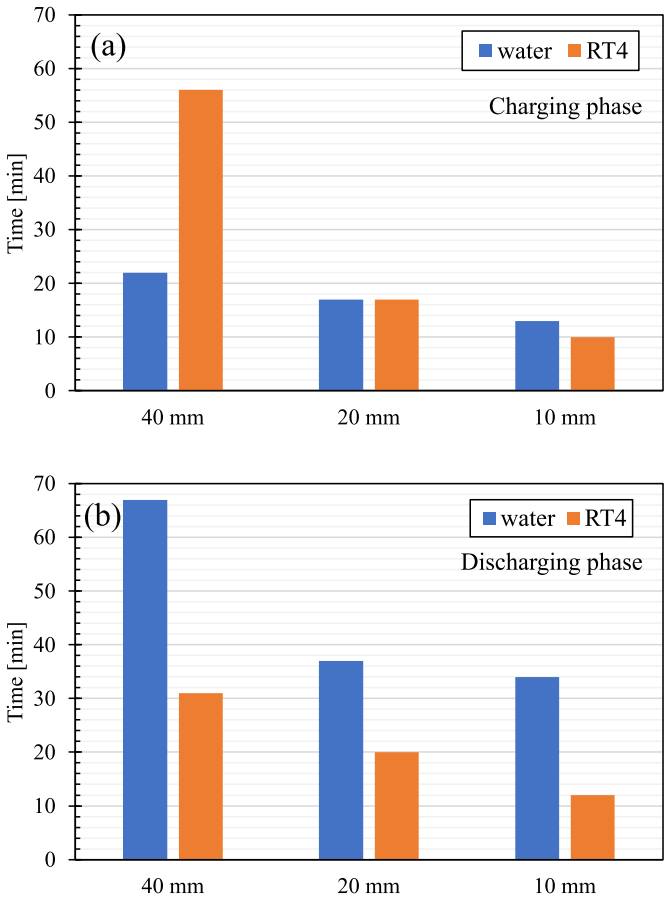

Fig. 5. Time required by water and RT4 to complete the charging (a) and discharging (b) phases when a d*t* of 9 K is applied.

behaviour with melting times around 21-22 min; RT5 presents a greater melting time due to its higher latent heat. The temperature profiles are similar for all these paraffin waxes but it is clear that the phase change process of the RT2 finished before all the others.

It is also very interesting to compare OM8 with CR9, two materials with similar t_{PC} but slightly different thermophysical properties: OM8 has lower latent heat (175 vs 220 kJ/kg) and lower solid specific heat capacity (1.71 vs 2.2 kJ/kg K). During charging, OM8 presents a remarkable subcooling by about 5 K and, once the solidification is started, the average temperature does not show any phase change plateau, while, in the case of CR9, no significant subcooling is observed and the temperature exhibits a well-defined plateau (about 28 min at almost constant temperature). The difference in the temperature behaviour can be attributed to the different heat transfer mechanism: the high value of the dynamic viscosity of the CR9 almost suppresses the natural convection and the heat transfer is controlled by the pure conduction. Unfortunately, the CR9 exhibits also the lowest solid thermal conductivity and thus the process is extremely slow. The dynamic viscosity of the OM8 is more than 2.5 times lower than that of CR9 and thus the natural convection may also play an important contribution to the phase change. During discharging, both materials display similar behaviour and require the same amount of time to complete the melting process. In general, the behaviour of the materials during the discharging phase, as represented by Fig. 6b, is more homogeneous: this can be explained considering that in the case of melting process, at the beginning the main heat transfer mechanism is the heat conduction and the natural convection becomes stronger as the liquid fraction increases. Water takes the longest time to complete the discharging process, around 37 min, because of its higher latent heat, while all other materials take between 20 and 26 min.

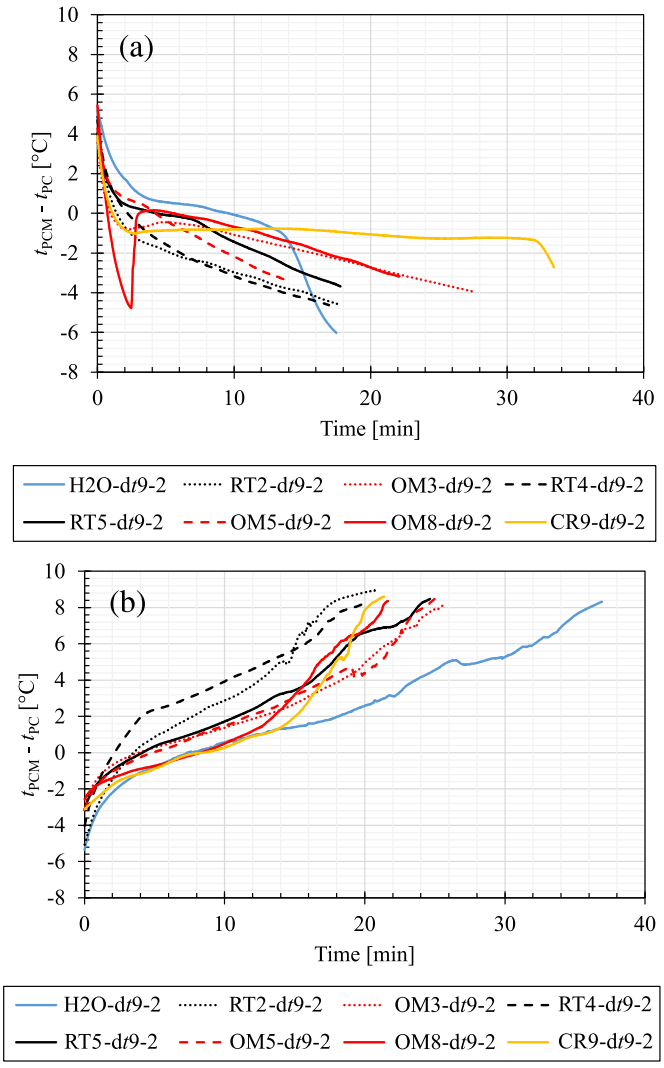

Fig. 6. Average temperature difference during the charging (a) and discharging (b) process of the 7 materials (plus water) in the 20 mm sample when the bath to t_{PC} temperature difference is kept equal to 9 K.

In general, it can be stated that in order to properly select the material, it is fundamental to investigate the behaviour of the very same material it is going to be used in the application because all its thermophysical properties deeply affect its heat transfer behaviour during the phase change process. The results clearly show that it is not possible to use data from other materials with similar phase change temperature to estimate the dynamic performance of the thermal storage without taking the risk of misleading results.

4.2. *Effect of the working conditions*

Fig. 7 reports the average temperature difference between the PCM and its t_{PC} over time as a function of the temperature difference between the thermal bath and t_{PC} (d*t*). In detail, it presents the charging phase of RT5 and OM5 at temperature differences d*t* equal to 3, 6, and 9 K in the 10 mm sample. RT5 and OM5 are both paraffin waxes and, as expected, they present similar heat transfer behaviour.

From the plotted results, it appears that when the d*t* is halved (from 6 K to 3 K) the phase change time on average present an increment by about 2.6 times. Furthermore, when the d*t* becomes one-third (from 9 K to 3 K) the phase time is about 4 times longer. Comparing the data in Tables 3, 4, and 5, it can be calculated that the trend is approximately common to all conditions tested. As might be expected, it is advisable to

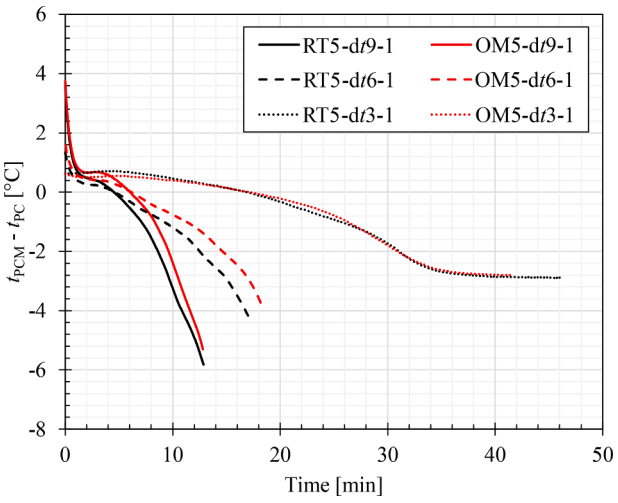

Fig. 7. Average temperature difference during the charging phase of RT5 (black) and OM5 (red) at the bath to t_{PC} temperature difference equal to 3, 6, and 9 K in the 10 mm sample.

select a PCM that permits to work with large d*t*, to reduce charging and discharging times. On the other hand, however, the higher energy requirements of producing much colder (or hotter) water must be kept in mind. In general, it might be suggested not to reduce the d*t* below 5 K as also found by Righetti et al. (2022), which has been found to be the minimum value to guarantee an efficient heat transfer on PCM side.

4.3. Local temperature field analysis

For space constrains, this section considers just one material (RT2) and analyses the temperature field inside it during the test carried out at d*t* 9 K in the reference and 10 mm samples. The location of the thermocouples (TCs) described in the following lines is shown in Fig. 3.

Fig. 8 shows the temperature profiles during the charging (Fig. 8a and c) and discharging phase (Fig. 8b and d) of reference (Fig. 8a and b) and 10 mm (Fig. 8c and d) samples.

As expected, a tendency for a radial heat transfer is observed. In fact, during the charging phase of RT2 in the reference sample, Fig. 8a, the first TCs to cool down and complete the phase change are TC1 and TC4, which are located near the walls. Then, TC2 and TC5, which are placed in the centre of the specimen, solidify. TC3 is not presented since, due to volumetric expansion and shrinkage, it measures the temperature of the surface in contact with air.

In the 10 mm sample, Fig. 8c and d, it can be seen that TC2, located in the centre of the sample, completes the solidification earlier than TC5 but TC2 is closer to an aluminium ligament where the heat transfer is enhanced. Similar behaviour occurs during the discharging phase and this behaviour is common to all the investigated materials.

It clearly appears that lattice shortens the charging and discharging times but, as said previously, it has a stronger enhancement in the charging (i.e., solidification) phase. Besides, the temperature is more homogeneous in the 10 mm sample if compared to the reference one: observe Fig. 8a versus Fig. 8c (charging) and Fig. 8b versus Fig. 8d (discharging). The difference between the minimum and maximum temperature recorded at the same time is around 2.3–2.5 K lower in the 10 mm sample. In general, to achieve a shorter phase change process and a more homogeneous temperature field, it is always recommended to use a metal structure, (Righetti et al., 2020a, 2020b).

5. Conclusions

Seven different commercially available phase change materials (PCMs) having nominal phase change temperatures (t_{PC}) between 2 and 9 °C were compared in 4 different samples subjected to cooling and heating conditions thanks to the immersion in thermostatic baths set at different temperatures. Several experimental tests were conducted to

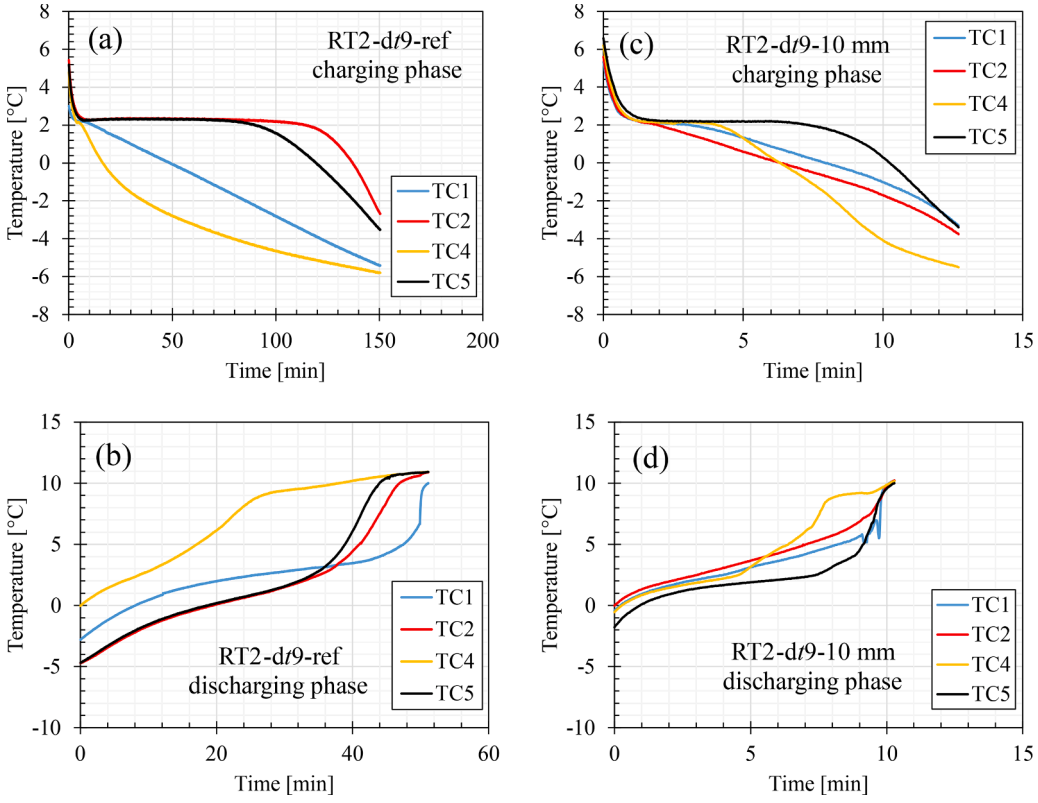

Fig. 8. RT2 temperature field in the reference (a, b) and 10 mm (c, d) samples during the charging (a, c) and discharging (b, d) phases run with d*t* 9 K.

study compatibility of the PCMs with a few common materials as well as the PCM temperature field and total charging and discharging times during the phase change.

From the collected results, it can be stated what follows.

- With rare exceptions, all the materials analysed seem to be compatible with the common construction materials used in the test rigs, industrial plants and machines (i.e., aluminium, copper, stainless steel and plastic).
- The duration of phase change depends not only on latent heat, but also on the other thermophysical properties, such as thermal conductivity and dynamic viscosity. The average temperature does not vary in the same way in different materials. Some materials exhibit subcooling, others do not, despite being all organic materials. Some have a very pronounced plateau zone during phase change, others do not. So, it is strongly recommended to study beforehand the very same material it is going to be used instead of to extrapolate information from data of different materials with similar phase change temperatures. Moreover, it is also suggested to collect all the available thermo-physical properties to accurately design the TES for a given application.
- When the temperature difference between thermostatic bath and t_{PC} (dt) is halved (from 6 K to 3 K) the charging time is reduced by an average of 160%, while when the dt becomes one-third (from 9 K to 3 K) the charging time is reduced by about 3 times. As might be expected, it is advisable to work with large dt to reduce operation times. On the other hand, however, one must keep in mind the higher energy expense of producing much colder (or hotter) water; in general, a dt at least of 5 K can be considered the proper trade-off between the storage performance and the system efficiency.
- The presence of a metal structure reduces both charging and discharging times. Under the same operating conditions, the time of the charging process is reduced more than the time of the discharging process. In addition, not all materials are subject to the same reduction in phase change time as the geometry of lattice structures changes and this evidence can be explained to the different thermophysical properties. Among those tested, the PCM that is most sensitive to lattice geometry are RT2 and RT4, some of the materials having the lowest thermal conductivity. On the other hand, the least sensitive material is water which has the highest values of solid and liquid thermal conductivity.
- As expected for the investigated boundary conditions, a radial heat transfer is observed within the sample. The presence of the 3D aluminium structure makes the temperature field more homogeneous.

In conclusion, the data presented can provide information currently unavailable in the literature and encourage designers to use PCMs in low-temperature applications as well. In addition, to achieve a shorter phase change process and a more homogeneous temperature field, it is always recommended to use a metal structure. Finally, the present results highlight how the thermo-physical properties of the studied PCMs deeply affect the phase change behaviour and thus they clearly demonstrate how inaccurate can be the predictions and the designs based on partial material properties data. Additional, work must be done to collect and publish the transport properties, such as thermal conductivity and dynamic viscosity of different PCMs to build a robust and comprehensive international database.

Declaration of Competing Interest

The authors declare that they have no known competing financial interests or personal relationships that could have appeared to influence the work reported in this paper.

Acknoledgments

This research work was partly funded by the PRIN 2017 FlexHeat 2017KAAECT project.

References

Al-Maghalseh, M., Mahkamov, K., 2018. Methods of heat transfer intensification in PCM thermal storage systems: review paper. Renew. Sustain. Energy Rev. 92, 62–94. https://doi.org/10.1016/J.RSER.2018.04.064.

Calati, M., Hooman, K., Mancin, S., 2022. Thermal storage based on phase change materials (PCMs) for refrigerated transport and distribution applications along the cold chain: a review. Int. J. Thermofluids 16, 100224. https://doi.org/10.1016/j.ijft.2022.100224.

Dong, X., Gao, G., Zhao, X., Qiu, Z., Li, C., Zhang, J., Zheng, P., 2022. Investigation on heat transfer and phase transition in phase change material (PCM) balls and cold energy storage tank. J. Energy Storage 50. https://doi.org/10.1016/j.est.2022.104695.

Kalapala, L., Devanuri, J.K., 2018. Influence of operational and design parameters on the performance of a PCM based heat exchanger for thermal energy storage – a review. J. Energy Storage 20, 497–519. https://doi.org/10.1016/J.EST.2018.10.024.

Khan, Z., Khan, Z., Ghafoor, A., 2016. A review of performance enhancement of PCM based latent heat storage system within the context of materials, thermal stability and compatibility. Energy Convers. Manag. 115, 132–158. https://doi.org/10.1016/J.ENCONMAN.2016.02.045.

Li, G., Hwang, Y., Radermacher, R., 2012. Review of cold storage materials for air conditioning application. Int. J. Refrig. 2053–2077. https://doi.org/10.1016/j.ijrefrig.2012.06.003.

Liu, Y., Zheng, R., Li, J., 2022. High latent heat phase change materials (PCMs) with low melting temperature for thermal management and storage of electronic devices and power batteries: critical review. Renew. Sustain. Energy Rev. https://doi.org/10.1016/j.rser.2022.112783.

Longo, G.A., Mancin, S., Righetti, G., Zilio, C., 2022. Experimental measurement of thermophysical properties of some commercial phase change materials (PCM) for air conditioning applications. Int. J. Refrig. https://doi.org/10.1016/j.ijrefrig.2022.08.007.

Mahdi, J.M., Lohrasbi, S., Nsofor, E.C., 2019. Hybrid heat transfer enhancement for latent-heat thermal energy storage systems: a review. Int. J. Heat Mass Transf. 137, 630–649. https://doi.org/10.1016/J.IJHEATMASSTRANSFER.2019.03.111.

Maiorino, A., del Duca, M.G., Mota-Babiloni, A., Greco, A., Aprea, C., 2019. The thermal performances of a refrigerator incorporating a phase change material. Int. J. Refrig. 100, 255–264. https://doi.org/10.1016/j.ijrefrig.2019.02.005.

Mehling, H., Brütting, M., Haussmann, T., 2022. PCM products and their fields of application - an overview of the state in 2020/2021. J. Energy Storage 51, 104354. https://doi.org/10.1016/J.EST.2022.104354.

Pirdavari, P., Hossainpour, S., 2020. Numerical study of a Phase Change Material (PCM) embedded solar thermal energy operated cool store: a feasibility study. Int. J. Refrig. 117, 114–123. https://doi.org/10.1016/j.ijrefrig.2020.04.028.

Qiao, Y., Du, Y., Muehlbauer, J., Hwang, Y., Radermacher, R., 2019. Experimental study of enhanced PCM exchangers applied in a thermal energy storage system for personal cooling. Int. J. Refrig. 102, 22–34. https://doi.org/10.1016/j.ijrefrig.2019.03.006.

Rakkappan, S.R., Sivan, S., Ahmed, S.N., Naarendharan, M., Sai Sudhir, P., 2021. Preparation, characterisation and energy storage performance study on 1-decanol-expanded graphite composite PCM for air-conditioning cold storage system. Int. J. Refrig. 123, 91–101. https://doi.org/10.1016/j.ijrefrig.2020.11.004.

Reddy, K.S., Mudgal, V., Mallick, T.K., 2018. Review of latent heat thermal energy storage for improved material stability and effective load management. J. Energy Storage 15, 205–227. https://doi.org/10.1016/J.EST.2017.11.005.

Rehman Ur, T., Ali, H.M., Janjua, M.M., Sajjad, U., Yan, W.M., 2019. A critical review on heat transfer augmentation of phase change materials embedded with porous materials/foams. Int. J. Heat Mass Transf. 135, 649–673. https://doi.org/10.1016/J.IJHEATMASSTRANSFER.2019.02.001.

Righetti, G., Doretti, L., Zilio, C., Longo, G.A., Mancin, S., 2020a. Experimental investigation of phase change of medium/high temperature paraffin wax embedded in 3D periodic structure. Int. J. Thermofluids 5-6, 100035. https://doi.org/10.1016/j.ijft.2020.100035.

Righetti, G., Savio, G., Meneghello, R., Doretti, L., Mancin, S., 2020b. Experimental study of phase change material (PCM) embedded in 3D periodic structures realized via additive manufacturing. Int. J. Therm. Sci. 153 https://doi.org/10.1016/j.ijthermalsci.2020.106376.

Righetti, G., Zilio, C., Buosi, A., Feo, D., Auerbach, M., Giannini, A., Butter, M., Mancin, S., 2022. Experimental assessment of a novel bio-based latent thermal energy storage for air conditioning. In: Proceedings of the 17th Conference on Sustainable Development of Energy, Water and Environment Systems (SDEWES), 06 - 10 November 2022 in Paphos, Cyprus.

Sarkar, S., Mestry, S., Mhaske, S.T., 2022. Developments in phase change material (PCM) doped energy efficient polyurethane (PU) foam for perishable food cold-storage applications: a review. J. Energy Storage. https://doi.org/10.1016/j.est.2022.104620.

Tao, Y.B., He, Y.L., 2018. A review of phase change material and performance enhancement method for latent heat storage system. Renew. Sustain. Energy Rev. 93, 245–259. https://doi.org/10.1016/J.RSER.2018.05.028.

Veerakumar, C., Sreekumar, A., 2016. Phase change material based cold thermal energy storage: materials, techniques and applications - a review. Int. J. Refrig. https://doi.org/10.1016/j.ijrefrig.2015.12.005.

Zhang, Z., Wang, D., Zhang, C., Chen, J., 2018. Electric vehicle range extension strategies based on improved AC system in cold climate – a review. Int. J. Refrig. https://doi.org/10.1016/j.ijrefrig.2017.12.018.